

THERMAL PERFORMANCE ANALYSIS AND OPTIMIZATION DESIGN OF DRY TYPE AIR CORE REACTOR WITH THE DOUBLE RAIN COVER

FaTing YUAN^{a,b}, ShouWei YANG^a, ShiHong QIN^c, Kai LV^a, Bo TANG^a, ShanShan HAN^d

a College of Electrical Engineering & New Energy, China Three Gorges University, Yichang, China

b Hubei Provincial Engineering Technology Research Center for Power Transmission Line, China Three Gorges University, Yichang, China

c School of electrical engineering and information, Wuhan Institute of Technology, Wuhan, China

d Medical College, China Three Gorges University, Yichang, China

Corresponding author: Shanshan Han (E-mail: feihu.1991@163.com).

In this paper, a fluid-thermal coupled finite element model is established according to the design parameters of dry type air core reactor. The detailed temperature distribution can be achieved, the maximum error coefficient of temperature rise is only 6% compared with the test results of prototype, and the accuracy of finite element calculate method is verified. Taking the equal height and heat flux design parameters of reactor as research object, the natural convection cooling performance of reactor with and without the rain cover is investigated. It can be found that the temperature rise of reactor is significantly increased when adding the rain cover, and the reasons are given by analyzing the fluid velocity distribution of air dcuts between the encapsulation coils. In order to reduce the temperature rise of the reactor with the rain cover, the optimization method based on the orthogonal experiment design and finite element method is proposed. The six factors of the double rain cover are given, which mainly affect the temperature rise of reactor, and the five levels are selected, the influence curve and contribution rate of each factor on the temperature rise of reactor are analyzed. The results show that the contribution ratio of the parameter H_1 , L_1 and L_2 , are obviously higher than the parameter H_2 , L_3 and θ , so the more attention should be paid in the design of double rain cover. Meanwhile, the optimal structural parameters of rain cover are given based on the influence curves, and the temperature rise is only 43.25°C. The results show that the optimization method can reduce the temperature rise of reactor significantly. In addition, the temperature distribution of inner encapsulations coils of reactor are basically the same, the current carrying capacity of coils can be fully utilized, which provides an important guidance for the optimization design of reactor.

Key words: *fluid-thermal coupled; dry type air core reactor; temperature rise, natural convection cooling, rain cover, orthogonal experiment design*

1. Introduction

The dry type air core reactor becomes the first type for large power reactor because of its simple structure, good linearity, light weight and high mechanical strength [1, 2]. It encounters overheating and even fire in the running process in recent years, and it have been confirmed that the partial high temperature of coils is one of the main reasons [3, 4]. Recently, the rain cover is often added at the top of reactor, to reduce the influence of external environment [5]. However, the heat dissipation conditions of coils gets worse after adding the rain cover, and partial encapsulation temperature rise may exceed the limit, which leads to the insulation and mechanical properties of the material changed, and consequently affects the safe and stable operation of the reactor in the power system. Thus, in order to reduce the influence of rain cover on temperature rise of reactor, the temperature distribution and heat dissipation characteristics of reactor should be analyzed when adding the rain cover, and the optimization methods about reactor are needed.

Currently, the research mainly includes: (1) The temperature distribution and heat dissipation characteristics: in [6], the empirical formula is adopted to calculate the average temperature rise of the reactor. In [7], the average temperature rise method is introduced by calculating the resistance, which is widely used in industrial production, however, the accuracy is low and can not reflect the heat dissipation characteristics. In [8], the finite difference method is used, the convection heat transfer coefficient along the axial direction of the coils is given based on the heat transfer criterion formula, and the temperature distribution of reactor can be obtained, but the calculation accuracy depends on the convection heat transfer coefficient, which limits its actual application. In [9], the temperature rise of transformer winding is given by establishing the Takagi-Sugeno model, but the computational process is complex. In order to obtain detailed and accurate temperature distribution of reactor, the finite element method is used. In [10, 11], the 2D finite element model of reactor is established, and the detailed temperature field distribution is achieved. In [12], the 3D temperature field simulation model of reactor is established, the influence of the rain cover is considered, the results of prototype experiment verify the correctness of finite element method. However, the heat dissipation characteristics of reactor have not been considered when adding the rain cover. (2) The optimization methods about reactor: in [13], the finite element method is used to reduce the temperature rise of reactor by adjusting the air ducts width and the thickness of the coils. In [14, 15], the genetic algorithm and particle swarm optimization algorithm are applied to the design of the reactor, but the large computation and long time is needed. In [16], the encapsulation-air ducts unit optimization method is proposed, but the effect of air ducts width on the thermal efficiency is not considered. In [17], the structure parameters of the rain cover is achieved based on the engineering experience, but the accuracy is low. In [18], the rain cover is equivalent to tilting baffle model, the influence factors of rain cover on temperature rise of the reactor are analyzed, and the optimal structural parameters are given based on the finite element method, however, it is only applicable to the tilting baffle model, which limits its practical application. In [19], the FEM and Taguchi combined method is used to achieve the optimal structure parameters of sound arrester, but the situation of single rain cover is merely considered. In fact, the outline size of rain cover also has a great influence on the temperature rise. In [20], the double rain cover structure parameters are acquired in the forced air cooling conditions, it can realize the same fluid velocity distribution in the air ducts, and the heat dissipation efficiency can be improved. However, the above method fails to elucidate the influence law of rain cover on temperature rise of reactor, and the optimal structure parameter cannot be obtained.

In this paper, according to the design parameters of reactor, a fluid-thermal coupled finite element model is established based on ANSYS simulation platform. The temperature field simulation results are achieved, and the maximum temperature rise is 51.6°C . Meanwhile, the prototype temperature rise test is done and the temperature rise is 49°C , so the accuracy of finite element method is verified. In order to reduce the temperature rise of the reactor with the rain cover, taking the equal height and heat flux design parameters of reactor as research object, the six influence factors of the double rain cover on temperature rise of reactor are considered, and five levels are selected. Combined with the orthogonal experiment design and finite element method, it can be found the maximum temperature rise of inner encapsulations is higher after adding the rain cover, and the reasons are given by analyzing the fluid velocity distribution of air ducts. Meanwhile, the influence curve and contribution rate of each factor on the temperature rise are analyzed, and the optimal parameters of the rain cover are obtained. The results show that the optimization method can reduce the temperature rise of reactor significantly.

2. Temperature field simulation of reactor

2.1. The basic structure and parameters

The dry type air core reactor is mainly composed by the several coaxial encapsulation coils, which are parallel connected in electric, and the coils are composed by the metal conductor and insulating material. The sustaining bars locates the adjacent encapsulation coils, which acts as the insulation and heat dissipation channels. The upper and lower ends of the encapsulation coils are the spider arm, which plays a role of distributing current and strengthen coils. Fig. 1 is the basic structure and equivalent model of dry type air core reactor in natural cooling conditions. The main electric parameters of reactor are as follows: the inductance is 3.1 mH ; the rated current is 3150 A , the rated voltage is 220 kV . The main geometrical parameters of reactor are as follows: the height of coils is 1.75 m , the inner radius of coils is 0.3 m , the outside radius of coils is 1.1 m , the number of coils is 12 and the metal conductor material is aluminum. The double rain cover is added at the top of reactor, which includes the lower and upper rain cover. The heat generated by the encapsulation coils is dissipated through the bottom end of the lower rain cover and the central hole between the upper and lower rain cover, which has a better heat dissipation performance compared with the single rain cover.

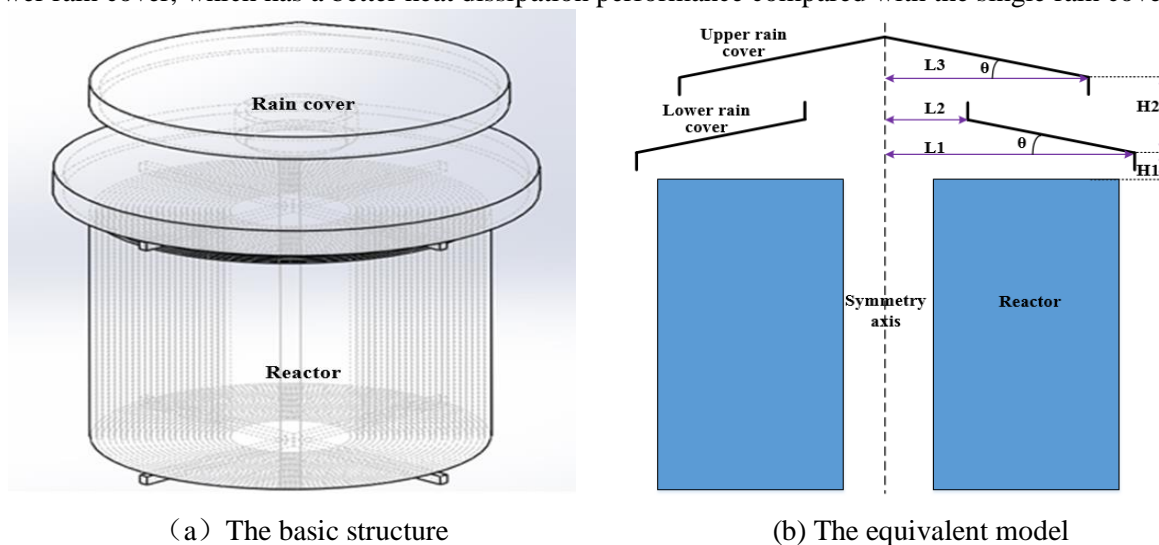


Figure 1. The basic structure and equivalent model of reactor

2.2. Loss calculation

The spider arm and sustaining bar have little influence on the temperature rise of reactor, thus, only the loss of the encapsulation coils should be considered in the calculation of temperature field. The loss of reactor mainly includes resistance loss and eddy current loss, which is the precondition for the temperature field simulation calculation.

Resistance loss of coils: the resistance loss, $P_{0,i}$, can be written as ^[21]:

$$P_{0,i} = I_i^2 \frac{\pi D_i W_i}{\kappa S_i} \quad (1)$$

Where, I_i 、 D_i 、 W_i and S_i are the current, diameter, turns number and conductor cross-section area of the encapsulation i respectively, κ is the conductivity of metal conductor.

Eddy current loss of coils: the eddy current loss, $P_{c,i}$, can be expressed as ^[22, 23]:

$$P_{c,i} = \frac{\pi W_i D_i \kappa \omega^2 a_i b_i}{12} (a_i^2 B_{z,i}^2 + b_i^2 B_{r,i}^2) \quad (2)$$

Where, ω is angular velocity, a_i 、 b_i are the radial width and single-turn axial height of the encapsulation i , $B_{z,i}$ and $B_{r,i}$ are the axial and radial component of the magnetic flux density. The magnetic flux density distribution of reactor depends on the diameter, height, turns number and current of the encapsulation coils, which can be achieved by analytical calculation method. Thus, the total loss of each encapsulation can be written as the sum of resistance loss and eddy current loss.

2.3. Temperature field simulation

In order to obtain the detailed and accurate temperature distribution, the FEM is selected considering the complex structure and heat dissipation process of the reactor with the rain cover. The temperature field simulation process mainly includes simulation model establishment, control equation, heat source loading, boundary conditions and grid generation.

2.3.1 Model establishment

According to the structural characteristic of reactor, the spider arm and sustaining bar, which interrupt the heat flow of coils, are relatively small compared with the total heat dispersing surface of coils ^[12], thus, the actual reactor with the encapsulation coils and double rain cover can be equivalent to 2D symmetrical axis model. The simulation model is established based on ANSYS simulation platform, as shown in Fig. 2. Some simplification and equivalent are done, only considering the steady-state thermal process, the encapsulation coils of reactor and double rain cover are equivalent to 2D axisymmetric model, the size of coils and double rain cover are basically identical to actual design parameters. Considering both the computation time and accuracy, the whole computational domain adopts the 2.5 times radial length and 3 times axial height of reactor in the model.

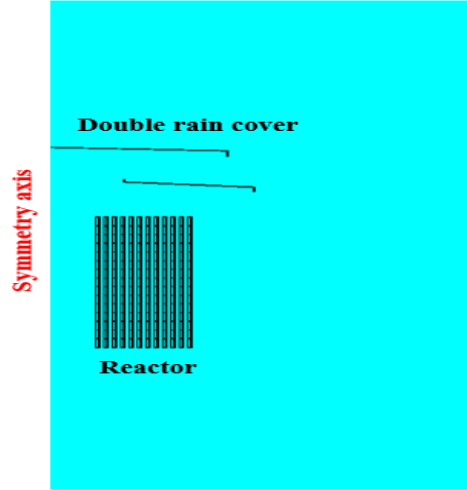


Figure 2. The Temperature field simulation model

The physical properties of metal conductor can be obtained according to the actual aluminum, the outer insulating material of metal conductor and rain cover are set as the same, as shown in Tab. 1. The region which around the coils and the rain cover is defined as the air, the physical properties can be achieved according to the corresponding pressure and temperature.

Table 1. The physical properties of material

Material	Density (kgm-3)	Thermal conductivity coefficient $Wm^{-1}K^{-1}$	Specific heat capacity $Jkg^{-1}C^{-1}$
Metal conductor	2707	217	880
Insulation materials	980	0.5	1125

2.3.2 Control equation

The heat generated by the encapsulation coils of reactor is mainly dissipated outward by three ways, heat conduction, heat convection and heat radiation ^[24-26].

Heat conduction: In the steady state, the energy transmits in the metal conductors and insulation material is by the way of heat conduction, the control equation can be described as:

$$\frac{1}{r} \frac{\partial}{\partial r} (\lambda r \frac{\partial T}{\partial r}) + \frac{\partial}{\partial z} (\lambda \frac{\partial T}{\partial z}) + q = 0 \quad (3)$$

Where T is temperature, q is heat generating rate per unit volume, r and z are the length of radial and axial direction, and λ is the thermal conductivity.

The interface between the insulating material and the metal conductor in the inner of encapsulation coils is satisfied:

$$\lambda_1 \frac{\partial T_1}{\partial n} = \lambda_2 \frac{\partial T_2}{\partial n} \quad (4)$$

Where, λ_1, λ_2 are the thermal conductivity, T_1, T_2 are the temperature of insulating materials and metal conductors respectively, n is interface normal.

Heat convection: the energy transmits, including the encapsulation surface and surrounding air, rain cover and surrounding air, are mainly by the way of heat convection, the control equation can be represented by continuity, momentum and energy equation, the detailed equation can be found in [18].

Heat radiation: The radiation of inner encapsulation coils can be ignored due to the temperature difference between the adjacent encapsulation coils is small, thus, only the radiation of internal surface of encapsulation 1 and external surface of encapsulation 12 are considered.

2.3.3 Heat source loading

Supposing the total heat source of each encapsulation coil is equal between the actual parameter of reactor and simulation model, so the equivalent current density, which applied to the metal conductor surface in the model, can be calculated, as shown in Eq. (5).

$$J_{ii} = \frac{J_i S_i W_i}{S_{tot}} \quad (5)$$

Where, J_{ii} is the equivalent current density, S_{tot} is the total area of metal conductor in the model. J_i , S_i and W_i are the current density, conductor cross-section area and turns number of the actual encapsulation i .

2.3.4 Boundary setting and grid generation

The boundary conditions are essential to calculate the temperature field of reactor, the detailed setting refers to the reference [27]. The grid density directly affects the calculation accuracy and time, considering the temperature field simulation results mainly focuses on the region that nearing the encapsulation coils and rain cover, thus, the grid is relatively dense when nearing the encapsulation coils and rain cover, and relatively sparse when the region is far away the encapsulation coils and rain cover, as shown in Fig. 3.

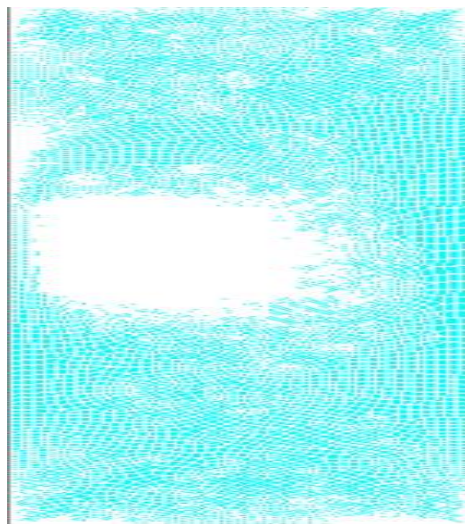


Figure 3. The grid generation of reactor

2.4. Temperature field simulation and test results

According to the parameters of reactor, the simulation model is established, and the temperature field simulation results are obtained by the material parameter setting, heat source loading, boundary condition setting and grid generation, as shown in Fig. 4.

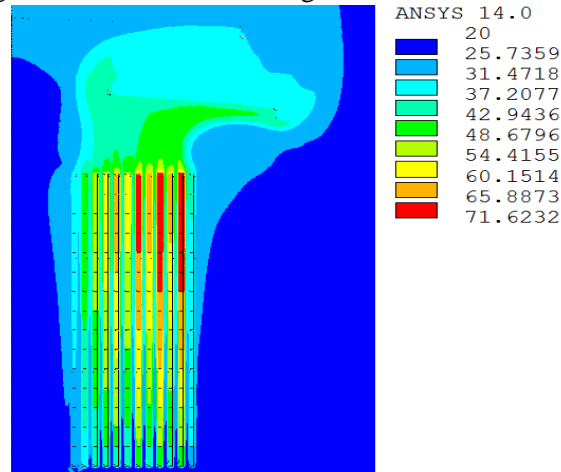


Figure 4. Temperature field simulation results

In Figure. 4, it shows that the maximum temperature rise is 51.6°C . At the same time, the grid-independence result test is carried out, the temperature rise under different grids are given in Tab. 2, it can be deduced that the temperature rise reached a stable value when the nodes number is 338432.

Table 2. The temperature rise under different grids

Number of nodes	116026	152799	200790	259341	338432
Temperature($^{\circ}\text{C}$)	70.9	71.0	71.3	71.6	71.6

The temperature rise test of prototype is done at the rated current, in the test, the thermal resistance is selected to measure the temperature rise of the reactor, it is attached to the surface of the wrapping coils, and the placement position of thermocouple is given in Fig. 5.

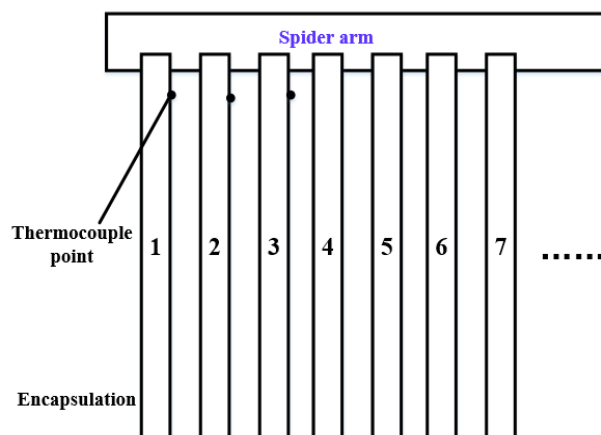
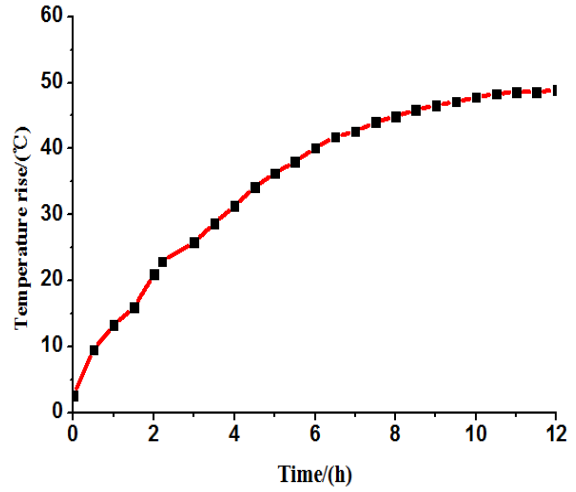


Figure 5. The placement position of thermocouple

The data of the maximum temperature rise is recorded every half hour, the prototype and temperature rise test results of reactor are given in Fig. 6, and the maximum temperature rise is gradually increased with the rise of the time, and tends to be stable within 12 hours.



(a) The prototype of reactor



(b) Test results

Figure 6. The prototype and temperature rise test results of reactor

In Fig 6, the measurement results show that the maximum temperature rise is about 49°C. the maximum error coefficient of temperature rise between the simulation results and test results is 5.3%, thus, the correctness of finite element method is verified.

3. Thermal characteristics analysis and optimization design of the double rain cover

The equal height and heat flux design method can realize the same temperature rise distribution for inner encapsulation without the rain cover, the carrying current capacity of reactor can be fully utilized [28,29], thus, this method is selected as research object to analyze the influence of rain cover on temperature rise. The main parameters of air core reactor are as follows: the rated inductance is 20.9 mH, rated current is 875.5 A, the encapsulation height is 1.75 m, the air ducts width are 0.025 m, encapsulation number is 12, and the inner radius of reactor is 0.3 m, the metal conductor material is aluminium.

3.1. Temperature field simulation results with the different rain cover

According to the structure characteristic of the double rain cover, the main factors which affecting the temperature rise of the reactor are six, they are L_1 , L_2 , L_3 , H_1 , H_2 and θ , thus, the above six factors are selected as the variables. Meanwhile, the accuracy will be reduced when the number of determined level is small, and the amount of computations is large and the computation time is long when the number of determined level is large. In order to balance the calculation accuracy and time, combined with the engineering experience, the five levels for each factor are selected, as shown in Tab. 3.

In Tab. 3, it exists 15625 ($5^6=15625$) different structural parameters of the double rain cover by permutation and combination method, in order to reduce the calculation amount and time, the orthogonal experimental design method is adopted in this paper, it is a method to study multi-factors and multi-levels by selecting some representative horizontal combinations, and finally find out the optimal horizontal combination based on the test results.

Table 3. The five level of each factor

Level	L_1 (m)	L_2 (m)	L_3 (m)	H_1 (m)	H_2 (m)	θ (deg)
1	0.90	0.20	0.60	0.100	0.30	10.0
2	0.95	0.25	0.65	0.125	0.35	12.5
3	1.00	0.30	0.70	0.150	0.40	15.0
4	1.05	0.35	0.75	0.175	0.45	17.5
5	1.10	0.40	0.80	0.200	0.50	20.0

Meanwhile, the orthogonal table, $L_{25}(5^6)$, is used based on the above factors and levels, and the simulation results with different structure parameters of double rain cover are given in Tab. 4. Where, the case 0 is defined as the temperature rise of reactor without the rain cover.

Table 4. Simulation results with the different rain cover

Case	L_1 (m)	L_2 (m)	L_3 (m)	H_1 (m)	H_2 (m)	θ (deg)	Temperature rise
0	—	—	—	—	—	—	46.32
1	0.90	0.20	0.60	0.100	0.30	10.0	72.57
2	0.90	0.25	0.65	0.125	0.35	12.5	63.80
3	0.90	0.30	0.70	0.150	0.40	15.0	58.79
4	0.90	0.35	0.75	0.175	0.45	17.5	55.88
5	0.90	0.40	0.80	0.200	0.50	20.0	53.70
6	0.95	0.20	0.65	0.150	0.45	20.0	58.93
7	0.95	0.25	0.70	0.175	0.50	10.0	57.39
8	0.95	0.30	0.75	0.200	0.30	12.5	55.76
9	0.95	0.35	0.80	0.100	0.35	15.0	58.23
10	0.95	0.40	0.60	0.125	0.40	17.5	56.35
11	1.00	0.20	0.70	0.200	0.35	17.5	55.22
12	1.00	0.25	0.75	0.100	0.40	20.0	57.02
13	1.00	0.30	0.80	0.125	0.45	10.0	56.76
14	1.00	0.35	0.60	0.150	0.50	12.5	55.29
15	1.00	0.40	0.65	0.175	0.30	15.0	55.51
16	1.05	0.20	0.75	0.125	0.50	15.0	57.12
17	1.05	0.25	0.80	0.150	0.30	17.5	56.18
18	1.05	0.30	0.60	0.175	0.35	20.0	56.23
19	1.05	0.35	0.65	0.200	0.40	10.0	53.30
20	1.05	0.40	0.70	0.100	0.45	12.5	55.33
21	1.10	0.20	0.80	0.175	0.40	12.5	55.29
22	1.10	0.25	0.60	0.200	0.45	15.0	53.71
23	1.10	0.30	0.65	0.100	0.50	17.5	55.14
24	1.10	0.35	0.70	0.125	0.30	20.0	58.57
25	1.10	0.40	0.75	0.150	0.35	10.0	53.68

In Tab. 4, it shows that the structure parameters of double rain cover have a great influence on temperature rise of reactor, in case 1, the maximum temperature rise is 72.57°C, but in case 19, the temperature rise is 53.30°C, they are significantly higher than the situation without the rain cover.

In order to analyze the reasons that the temperature rise of reactor is higher and different when adding the rain cover, the equivalent model and simulation results of case 1 and case 19 are selected, as shown in Fig. 7 and Fig. 8.

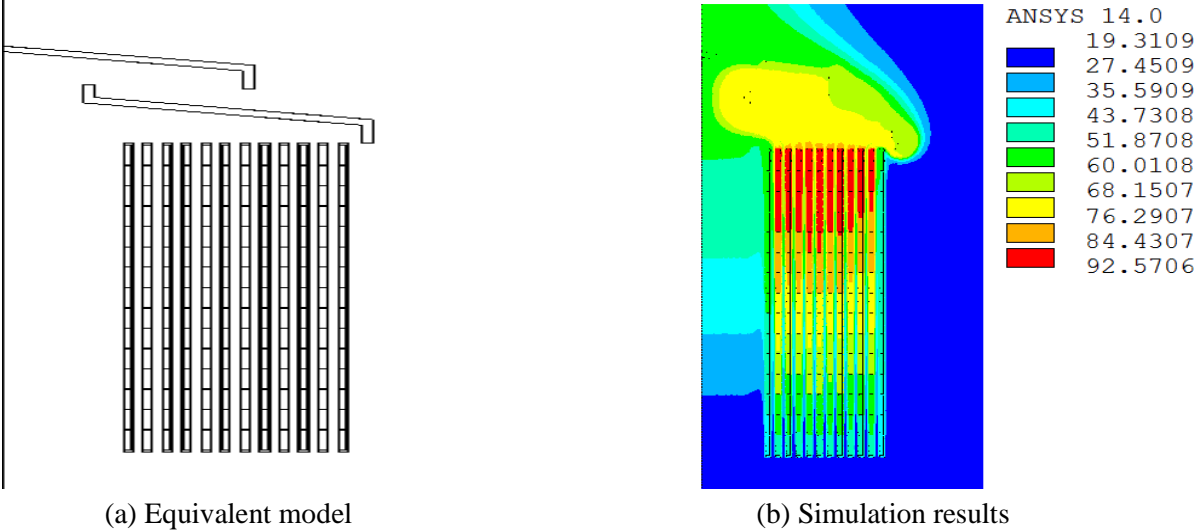


Figure 7. The equivalent model and simulation results in case 1

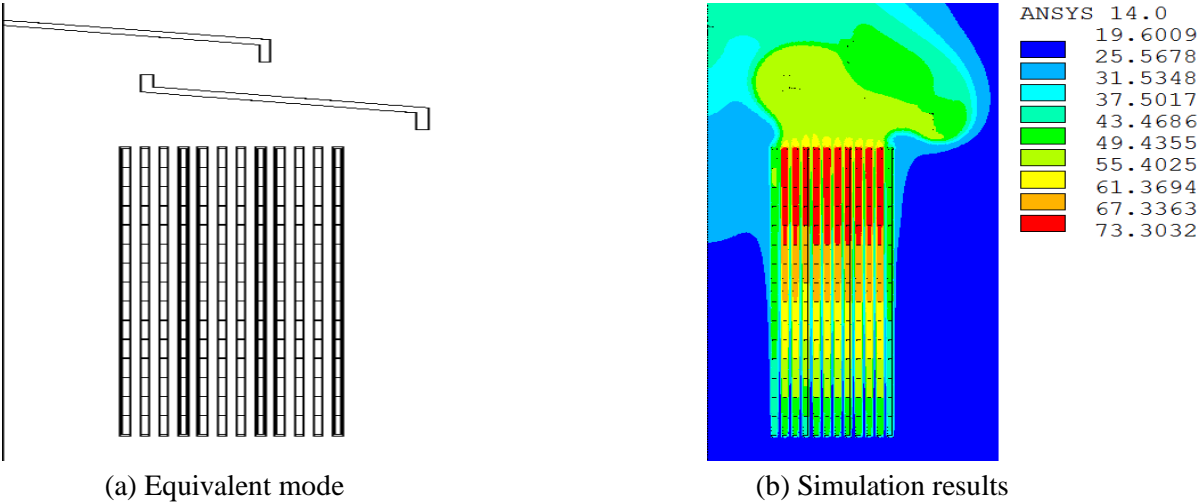


Figure 8. The equivalent model and simulation results in case 19

The extracted path of reactor is given based on the above simulation results, as shown in Fig. 9.

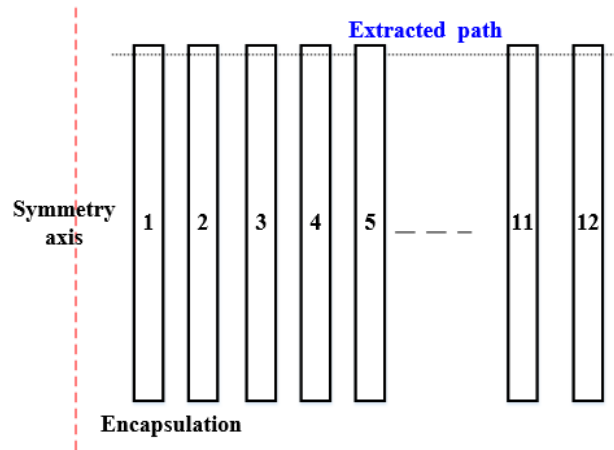


Figure 9. The extracted path of reactor

The temperature and axial fluid velocity distribution of the air ducts along the radial direction was extracted with the different case, as shown in Fig. 10.

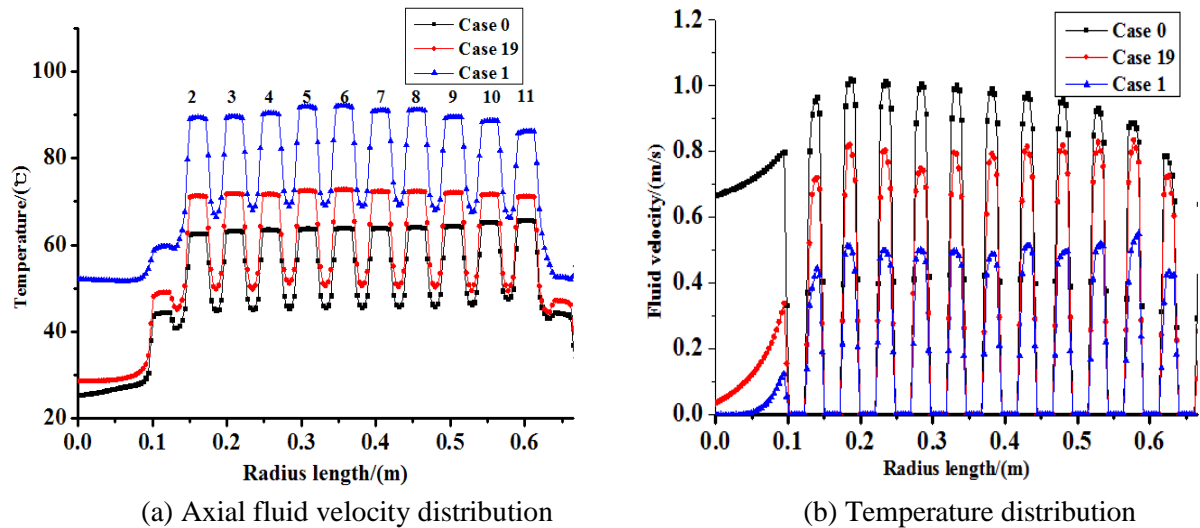


Figure 10. Axial fluid velocity and temperature distribution with the different case

In Fig. 10, it can be seen that the maximum temperature rise of inner encapsulation coils are basically the same, so the carrying ability can be efficiently utilized. Meanwhile, the maximum fluid velocity in the air ducts is 1.1m/s in case 0, however, when adding the double rain cover, the fluid velocity becomes the 0.5 m/s and 0.8 m/s in case 1 and case 19 respectively, so it can be concluded that the fluid velocity change leads to the temperature rise of the reactor increased.

3.2. Thermal performance characteristics analysis of the double rain cover

According to the temperature field simulation results with the different parameters, the performance statistics analysis results of the double rain cover can be obtained, as shown in Tab. 5.

Table 5. Performance statistics analysis of the double rain cover

Case	L_1 (m)	L_2 (m)	L_3 (m)	H_1 (m)	H_2 (m)	θ (deg)
PS_1	304.74	299.13	294.15	298.29	298.59	293.70
PS_2	286.66	288.10	286.68	292.60	287.16	285.47
PS_3	279.80	282.68	285.30	282.87	280.75	283.36
PS_4	278.16	281.27	279.46	280.30	280.61	278.77
PS_5	276.39	274.57	280.16	271.69	278.64	284.45
R_j	28.35	24.56	14.69	26.60	19.95	14.93

In Tab. 5, The calculation procedure of PS can be explained by an example, PS_1 is equal to the sum of temperature rise in level 1, which locates the row from case 1 to case 5.

The parameter, R_j , is defined as: ^[10]

$$R_j = (\max(PS_L) - \min(PS_L)) / 5 \quad L = 1, 2, 3, \dots, 5 \quad (6)$$

Where, j stands for the six undermined factors, L is the corresponding level of each parameter.

The total range is:

$$R_{sum} = R_{L_1} + R_{L_2} + R_{L_3} + R_{H_1} + R_{H_2} + R_{\theta} \quad (7)$$

The contribution ratio is defined as the Eq. (8), which indicates the influence degree of each parameters on temperature rise of the reactor.

$$Co_j = R_j / R_{sum} \quad (8)$$

From the Eq. (8), the contribution rate of each parameters can be plotted, as shown in Fig. 11.

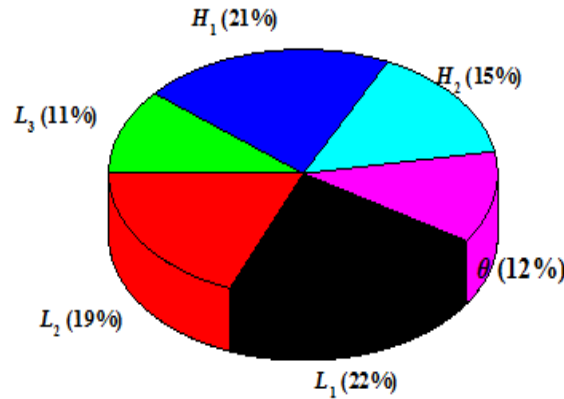
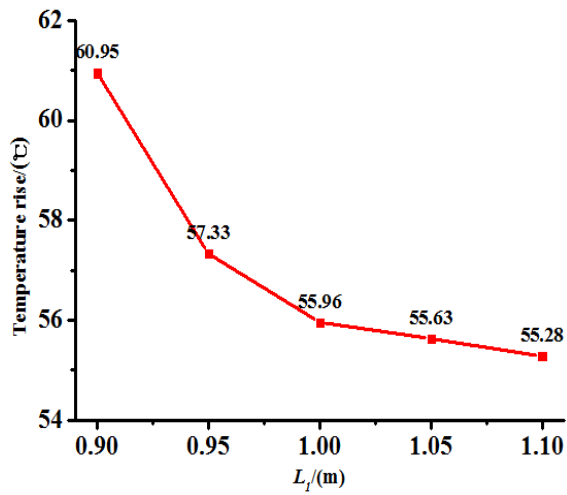


Figure 11. The contribution ratio of each parameter

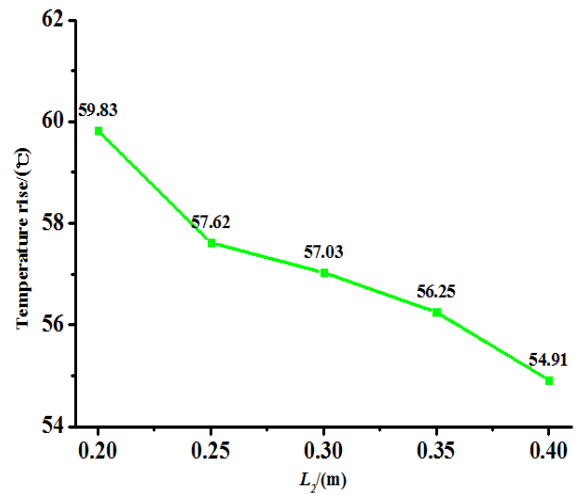
In Fig. 11, it can be found that the contribution ratio of parameter H_1 , L_1 and L_2 are obviously higher than H_2 , L_3 and θ , thus, the more attention should be paid in the design of double rain cover.

3.3. Optimization design of the double rain cover

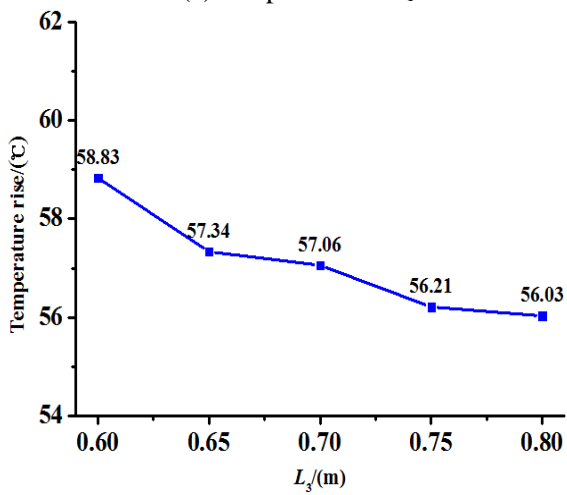
According to the simulation results in Tab.3, the curves is plotted, which reflects the effect of structural parameter variation on temperature rise of reactor, as shown in Fig. 12.



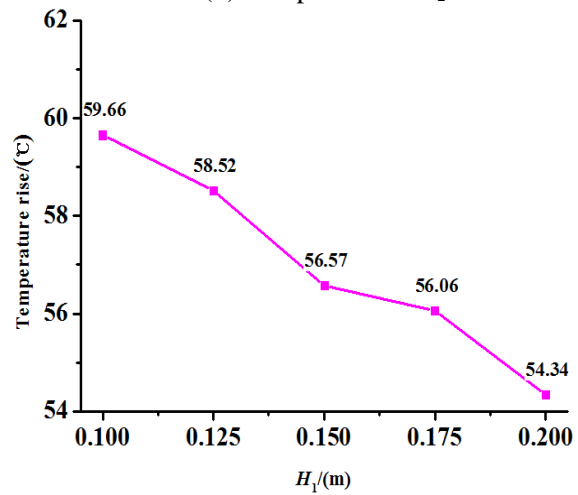
(a) The parameter L_1



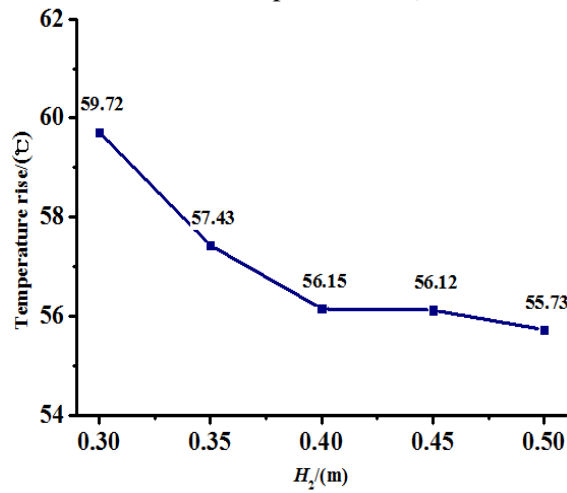
(b) The parameter L_2



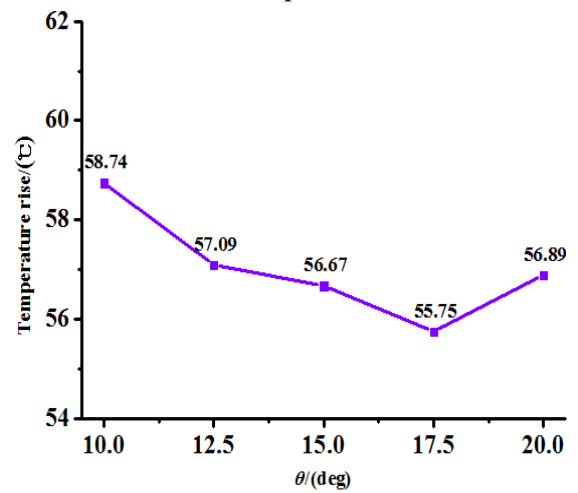
(c) The parameter L_3



(d) The parameter H_1



(e) The parameter H_2



(f) The parameter θ

Figure 12. The effect curves of each factor

In Fig. 12, it can be seen that the maximum temperature rise of reactor gradually decreased with the rise of the parameter L_1 , L_2 , L_3 , H_1 , H_2 and θ , the mainly reason is that the effect of the rain cover on the fluid velocity in the air ducts is decreased with the rise of the above parameters, the reactor has a better heat dissipation conditions and lower temperature rise. Meanwhile, it exists an inflection point in the parameter θ , when the value of θ continues to increase, it will hinder the fluid

flow between the lower and upper rain cover. Thus, the optimal parameter of double rain cover can be obtained when the temperature rise obtains the minimum in the curve, as shown in Tab. 6.

Table 6. The optimal parameters of the double rain cover

Parameter	L_1 (m)	L_2 (m)	L_3 (m)	H_1 (m)	H_2 (m)	θ (deg)
Value	1.1	0.4	0.8	0.2	0.5	17.5

According to the initial design parameters of reactor and the optimal structure parameter of the double rain cover, the temperature field simulation model is established, and the results is shown in Fig. 13.

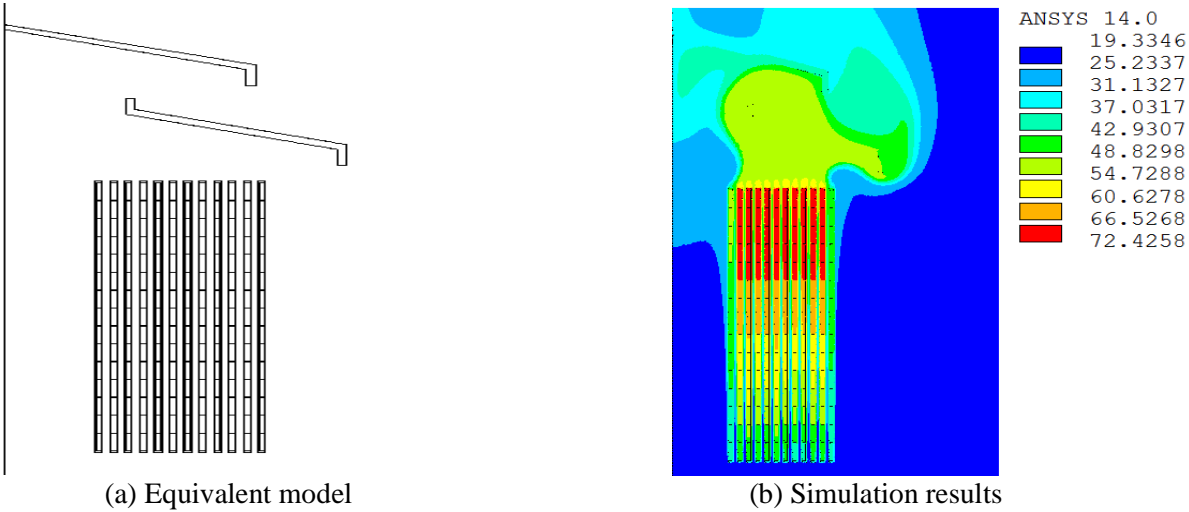


Figure 13. The equivalent model and simulation results with the optimization method

In Fig. 13, the maximum temperature rise of reactor is only 52.43°C, it is the minimum among the 25 different double rain cover structure parameter, thus, the simulation results verify the correctness of the optimization method. Meanwhile, the temperature distribution is extracted according to the simulation result, as shown in Fig. 14. It can be seen that the temperature rise distribution of inner encapsulations coils are basically the same under the optimal parameter of double rain cover.

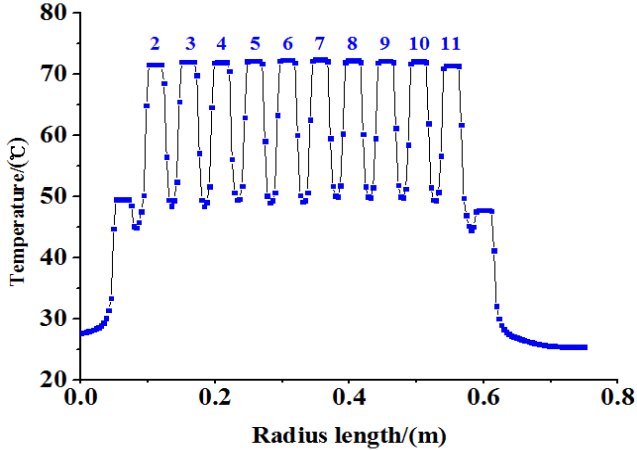


Figure 14. The temperature distribution with the optimization method

4. Conclusion

In this paper, a fluid-thermal coupled finite element model is established, the test results verified the accuracy of temperature field simulation calculation. Meanwhile, the orthogonal experimental method is adopted to analyze the influence laws of double rain cover on temperature rise of rain cover, and the following conclusions can be obtained.

(1) When adding the rain cover, the maximum temperature rise is changed from 46.32°C to 72.57°C, and the reasons are given by analyzing the fluid velocity distribution of air ducts between the encapsulation coils, the maximum fluid velocity of air ducts is changed from 1.1m/s to 0.5m/s without and with the rain cover.

(2) The influence curve and contribution rate of each factor on the temperature rise are analyzed, the contribution ratio of the parameter H_1 , L_1 and L_2 , are obviously higher than the parameter H_2 , L_3 and θ , so the more attention should be paid in the design of double rain cover. Meanwhile, the maximum temperature rise of reactor is only 52.43°C based on the optimal structural parameters of double rain cover, so the optimization method can obviously reduce the temperature rise of reactor.

(3) According to the simulation results, the temperature rise distribution of inner encapsulation coils are basically the same under the optimal parameters of double rain cover, the current carrying capacity of coils can be fully utilized, which provides an important guidance meaning for the optimization design of reactor.

Acknowledgment

This work was supported by the Natural Science Foundation of Hubei Province (No. 2020CFB376), Hubei Provincial Engineering Technology Research Center for Power Transmission Line Open Fund Project, China Three Gorges University (No. 2019KXL09), National Natural Science Foundation of China, (No. 51977121).

References

- [1] Liu, Z.G., *et al.*, The Optimum Design of Dry-type Air-Core Reactor, *High Voltage Engineering*, 29(2003), 2, pp. 17-20 (into Chinese)
- [2] Papp, K., *et al.*, High voltage dry-type air-core shunt reactors, *E & I Elektrotechnik und Informations technik*, 131(2014), 8, pp. 349-354
- [3] Liu, H. Y., Wei, B., Operation and Maintenance of Dry Air Core Reactor, *High Voltage Apparatus*, 40(2004), 3, pp. 239-241 (into Chinese)
- [4] Zhang, H., Cai, Y. L., Fault Analysis on Dry-type Air core Reactor in 500 kV Substation, *Power Capacitor and Reactive Power Compensation*, 37(2016), 1, pp. 46-50 (into Chinese)
- [5] Wang, P., *et al.*, Distribution of electric field and structure optimisation on the surface of a ± 1100 kV smoothing reactor, *IET Science, Measurement & Technology*, 13(2019), 3, pp. 441-446
- [6] Wu, S., Wu, D., Yan, S., A study of design and calculation method for dry-type reactor with air core, *Transformer*, 34(1997), 3, pp. 18-22 (into Chinese)

- [7] Ye, Z., Temperature Rise Test of Dry-Type Air-Core Reactor and Calculation of its Winding Temperature Rise, *Transformer*, 36(1999), 9, pp. 6-12 (into Chinese)
- [8] Wu, C. J., Investigation on the temperature distribution in a reactor and design of measure system by optical fiber sensor system, Master's thesis, Northwestern Polytechnical University, Xi'an, China, 2005
- [9] Xiong, H., Chen, W. G., Du, L., *et al.*, Study on Prediction of Top-oil Temperature for Power Transformer Based on T-S Model, *Chinese Journal of Electrical Engineering*, 27(2007), 10, pp. 15-19 (into Chinese)
- [10] Liu, Z. G., G, Y. S., W, J.H., *et al.*, Design and analysis of new type air-core reactor based on coupled fluid-thermal field calculation, *Transactions of China Electrotechnical Society*, 18(2003), 6, pp. 59-63 (in Chinese)
- [11] Yuan, F., Yuan, Z., Wang, Y., Thermal optimization for nature convection cooling performance of air core reactor with the rain cover. *IEEJ Transactions on Electrical and Electronic Engineering*, 13(2018), 7, pp. 995-1001
- [12] Jiang, Z. P., Wen, X.S., Wang, Y., *et al.*, Test and coupling calculation of temperature field for UHV Dry-type air-core smoothing reactor, *Proceedings of the CSEE*, 35(2015), 20, pp. 5344-5350 (in Chinese)
- [13] Smolka Jacek, Nowak Andrzej J., Shape optimization of coils and cooling ducts in dry-type transformers using computational fluid dynamics and genetic algorithm, *IEEE Transactions on Magnetics*, 47(2011), 6, pp. 1726-1731
- [14] Z Mohammed Sami Mohammed, Revna Acar Vural., NSGA-II+FEM based loss optimization of three phase transformer, *IEEE Transactions on Industrial Electronics*, 66(2019), 9, pp. 7417-7425
- [15] Bin, X., Gil-Gyun Jeong, Chang-Seop Koh., Co-kriging assisted PSO algorithm and its application to optimal transposition design of power transformer windings for the reduction of circulating current loss, *IEEE Transactions on Magnetics*, 52(2016), 3, pp. 1-4
- [16] Yuan F., Yuan Z., Chen L., *et al.*, Thermal and Electromagnetic Combined Optimization Design of Dry Type Air Core Reactor, *Energies*, 10(2017), 12, pp. 1989
- [17] WU, C. Z., Zhou, J. B., Zhao, J. M., *et al.*, Influence of rain and wind on Air-core reactor, *Power Capacitor and reactive Power Compensation*, 35(2014), 2, pp. 40-42+49 (in Chinese)
- [18] Yuan, F. T., Yuan, Z., Wang, Y., *et al.*, Thermal optimization for nature convection cooling performance of air core reactor with the rain cover, *IEEJ Transactions on Electrical and Electronic Engineering*, 7(2018), 13, pp. 995-1001.
- [19] Wang, Q. W., Chen, Q. Y., Zeng, M., A CFD-Taguchi combined method for numerical investigation of natural convection cooling performance of air-core reactor with noise reducing cover, *Numerical Heat Transfer Part A Applications*, 55(2009), 12 pp. 1116-1130
- [20] Deng, Q., Li, Z. B., Yin, X. G., *et al.*, Steady thermal field simulation of forced air-cooled column-type air-core reactor, *High Voltage Engineering*, 39(2013), 4, pp. 839-844

- [21] David, P., *et al.*, Comparison between BEM and classical FEM for a 3D low-frequency eddy-current analysis, *IEEE Transactions on Magnetics*, 46(2010), 8, pp. 2919-2922
- [22] Kurt, P., *et al.*, Eddy current losses in large air coils with layered stranded conductors, *IEEE Transactions on Magnetics*, 44(2008), 6, pp. 1318-1321
- [23] Yan, X.K., *et al.*, Research on calculating eddy-current losses in power transformer tank walls using finite-element method combined with analytical method, *IEEE Transactions on Magnetics*, 52(2016), 3, pp. 1-4
- [24] Wang, H., *et al.*, Numerical Calculation and Experimental Verification for Leakage Magnetic Field and Temperature Rise of Transformer Core Tie-Plate, *IEEE Transactions on Applied Superconductivity*, 29(2019), 2, pp. 1-5
- [25] Tsili, M., *et al.*, Power transformer thermal analysis by using an advanced coupled 3D heat transfer and fluid flow FEM model, *International Journal of Thermal Sciences*, 53(2012), pp. 188-201
- [26] Santisteban, A., *et al.*, Thermal Modelling of a Power Transformer Disc Type Winding Immersed in Mineral and Ester-Based Oils Using Network Models and CFD, *IEEE Access*, 7(2019), pp. 174651-174661
- [27] Yuan, Z., *et al.*, Thermal Analysis of Air core Power Reactors, *ISRN Mechanical Engineering*, (2013) pp. 1-6
- [28] Yuan, F.K., *et al.*, Optimization Design of Oil-Immersed Air Core Coupling Reactor for a 160 kV Mechanical Direct Current Circuit Breaker, *Energies*, 12(2019), 6.
- [29] Yuan, F.K., *et al.*, Optimization Design of a High-Coupling Split Reactor in a Parallel-Type Circuit Breaker, *IEEE Access*, (2019), 7, pp. 33473-33480.

Paper submitted: 14.10.2020

Paper revised: 18.01.2021

Paper accepted: 20.01.2021